Investigation of Signal Conditioning for Tx-Rx PEC Probe at High Lift-off Using a Modified Maxwell's Bridge

Denis Ijike Ona, Gui Yun Tian and Syed Mohsen Naqvi
School of Engineering, Newcastle University, United Kingdom NE1 7RU

Abstract— **Pulsed eddy current testing is widely used because of its richness in spectral components. However, the degrading sensitivity as lift-off increases poses a challenge to its application in thick insulation or buried structures and weld areas. In the transmitter-receiver probe, self-impedance (offset) of receiver coil dominates the output signal, reducing the signal-to-noise ratio, especially at high lift-off. This limits the subsequent amplification of the output signal by the signal conditioning circuit. In practice, bridge-based measurements are used to mitigate this challenge but result in small linear range input-output characteristics. Electromagnetic interference and stray capacitance effects also cause measurement errors. This paper investigates a modified Maxwell's inductance bridge based on operational amplifier configuration for high lift-off testing. The receiver coil self-impedance is removed to improve signal-to-noise ratio and to make output signal proportional to impedance change only. Experiments are performed to evaluate the performance of the circuit in crack detection. The results show improved signal-to-noise ratio with maximum linearity deviation of 0.30%, and a higher crack detection sensitivity at 30mm high lift-off, in comparison to the conventional bridge circuit with maximum linearity deviation of 0.53%.**

Index Terms—**Lift-off, Self-impedance, Signal conditioning, Transmitter-receiver probe.**

I. INTRODUCTION

Whereas, several techniques have been investigated for defect detection of conductive materials, the pulsed eddy current (PEC) technique, especially the detector coil-based PEC sensor configuration has been commonly used [1, 2]. Harsh environment tolerance, low cost, and rich spectral components are the attractive features of PEC [3]. The main reason for associating with transmitter-receiver (Tx-Rx) coil-based PEC sensors, is the possibility to optimize Tx and Rx (coils) separately [4, 5]. Another potential of (Tx-Rx) PEC probe is improved signal-to-noise ratio (SNR) with changing lift-off [6]. A Tx-Rx PEC system is a transformer with variable mutual couplings. Many factors cause the coupling to vary including samples, discontinuity, crack, metal loss and lift-off. These variations make up what Rx coil detects, as an impedance change or by a magnetic sensor as magnetic field change. However, the decrease in SNR of Tx-Rx PEC probe, due to the weakening of mutual coupling as lift-off increases is the focus of this work. The output signal of Rx circuit is mainly dominated by self-impedance (self-inductance and internal resistance), of Rx (coil) of which, impedance change used for testing, is just a small fraction of the output signal especially at high lift-off [7, 8]. Typically, the variation in coil impedance falls in the range of 5% to 10% of the self-impedance [9]. The inherent self-inductance of the Rx (coil) is also one of the sources of nonlinearity in the Rx output signal [10]. Due to the self-impedance of the Rx (coil), in addition to multi-parameter influence, the required information is sometimes masked in noise. This limits the subsequent amplification of the output signal, which is the key in applications with a low SNR [11].

The impedance change can be converted into electrical signals such as current, voltage, frequency, and phase using different circuits. Such circuits include an amplitude modulation circuit [12], a frequency modulation circuit, and bridge circuits [13-15]. Frequency output sensors can also be used as signal conditioning through oscillation for instance as in [10, 16, 17]. However, to balance the influence of coil self-impedance and improve sensitivity, bridge circuits are normally used as part of signal conditioning to convert the impedance change or magnetic field change into electrical signal [18]. Ac bridge circuit is operated in a balanced mode to null the offset due to self-impedance of Rx (coil) and to detect the impedance change as the balance is disturbed. Conventional ac bridges including Maxwell's inductance bridge, Anderson Bridge, Hay's bridge, etc. are used for this purpose [19]. However, a setback of bridge circuits is limited linear range input-output characteristic [20, 21]. Another setback of conventional bridges is the measurement error due to stray capacitance between bridge nodal point and ground, and stray inductance of the inductive coils [22]. Therefore, it is necessary to modify Maxwell's inductance bridge circuit that can remove the influence of self-impedance of the Rx (coil), reduce measurement errors, and improve SNR and linear input-output characteristics. Such a measurement circuit suitable for capacitive sensors with large offset capacitance has been presented in [23, 24]. In the circuit of [23], a sensing capacitor in a T-network is connected in a negative feedback loop of an operation amplifier (opamp), while a reference capacitor in another T-network is connected in a positive feedback loop of the same opamp. The output of the two networks are then fed to an instrumentation amplifier which gives zero output voltage when the two capacitance values are equal and non-zero output voltage when there is a difference between the two capacitance values arising from the change in the measured parameter. By this technique the large offset capacitance of a capacitive human proximity sensor is removed and detection sensitivity improved.

We borrow this idea by using two Rx (coils) in the feedback networks of opamp. The outputs of the two Rx (coils) are fed to the subtractor opamp. The subtractor gives zero output voltage when the two impedance values are equal and non-zero voltage when there is a difference in impedance values. Based on this idea, we propose a simple circuit that removes the large self-impedance of Rx (coil) using opamp based bridge circuit. This circuit can be seen as a modified Maxwell's inductance bridge considering the arrangement of the passive components of the circuit (Fig. 3). The major aim is to remove the effect of self-impedance of the Rx (coil) from

Manuscript received, revise, Accepted, date of publication, date of current version. The work of Denis Ijike Ona is supported by the Nigeria Tertiary Educational Fund. The authors are with School of Engineering, Newcastle University, United Kingdom NE1 7RU. (e-mail: D.I.Ona@newcastle.ac.uk; G.Y.Tian@ncl.ac.uk; mohsen.naqvi@newcastle.ac.uk)

the mutual impedance of the PEC probe and the test sample. We use part of the circuit of [25] which consists of two inverting opamps and a subtractor circuit to configure two Rx coils. Two Rx coils form the feedback loops of the two inverting opamps with both coils coupled to the Tx (coil). Adopting the linear variable differential transformer approach [26], the two Rx (coils) are arranged into a push-pull configuration. That is the mutual inductance of Tx and one coil of Rx is made positive, while the mutual inductance of Tx and another coil of Rx is made negative through coil winding. Hence, the difference between the mutual inductances of the two Rx (coils) and Tx (coil) becomes twice that of one Rx (coil). The remaining part of the paper is organized as follows. In Section II, the influence of mutual inductance and self-impedance of the Rx (coil) including lift-off influence on output signal of the equivalent circuit of Tx-Rx is analyzed. Section III describes the proposed signal conditioning circuit. Section IV analyses different sources of error of the circuit. Section V is on an experimental study. Section VI discusses the experimental results and comparison of the circuits. Finally, Section VII derives the conclusion and highlights future work.

II. Analysis of Equivalent Circuit of Tx-Rx PEC Probe

To understand how self-impedance of Rx (coil) dominates the output signal of Tx-Rx PEC probe which leads to low SNR especially at high lift-off, we analyze the equivalent circuit of Tx-Rx PEC probe. Mutual inductance based PEC probe depends on the linking magnetic field of coils and sample. Time changing voltage or current in the Tx (coil) generates magnetic flux that couples both directly and indirectly through the sample with Rx (coil). The equivalent circuit used to induce and extract the induced voltage from the Rx (coil) is in Fig. 1. We analyze the circuit without a sample and then introduce a sample and modify the circuit to include the influence of the sample. Without a sample as in Fig. (1a), the proximity of the Tx and Rx equivalent circuit results in a mutual inductance of Tx and Rx ,where the mutually induced electromotive force (EMF) is given by the following equations.

$$\varepsilon_1 = -M_{12}\frac{di_2}{dt} \quad (1)$$

$$\varepsilon_2 = -M_{21}\frac{di_1}{dt} \quad (2)$$

$$L_1\frac{di_1}{dt} + (r_1 + Rs\ )i_1 = M\frac{di_2}{dt} + V_sU(t) \quad (3)$$

$$L_2\frac{di_2}{dt} + (r_2 + R_L)i_2 = M\frac{di_1}{dt} \quad (4)$$

M = Direct mutual inductance of Tx and Rx
$\mathcal{M}$ = Mutual inductance of Tx and Rx through Sample
Vs = Excitation voltage
V_0 = Rx output Voltage
L_1, L_2= Self-inductance of Tx and Rx
r_1, r_2 = Internal resistance of Tx and Rx (coils)
R_s = Source resistance
R_L = Load resistance
$\mathcal{L}_1$, $\mathcal{L}_2$= self-couplings of Tx and Rx (coils) through the sample
i_1, i_2 = Tx and Rx current
$\mathcal{E}_1$, $\mathcal{E}_2$ = Mutually induced EMF of Tx and Rx
M_{12}, M_{21} = Mutual inductance due to the current change in Rx and Tx

M_{12}= M_{21} = M

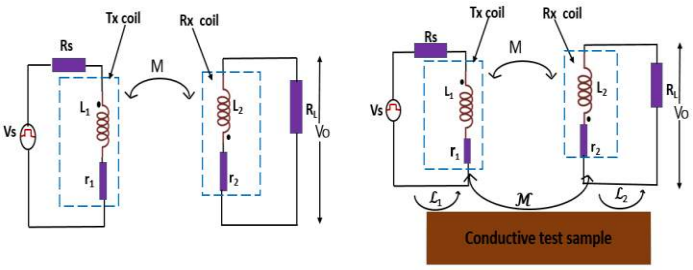

Fig. 1. Tx-Rx equivalent circuit (a) without sample (b) with sample

In proximity to a sample as in Fig. 1b, the magnetic field developed by the probe induces eddy currents (EC) in a nearby conductive sample. The EC in the sample develop an opposing magnetic field that generates an additional EMF in both coils following Lenz's law [27-29].While the Tx (coil) generates an electromagnetic field [30], the Rx (coil) measures the reflected field from the test sample as the voltage across the load resistance RL [31]. It is from the induced voltage in the Rx (coil) that the status of the test sample is evaluated. However, the total field in the presence of a sample can be considered as a sum of the original field of the coil in the air plus a reflected field from the metal sample [11, 32, 33]. In presence of a sample to a Tx-Rx probe, there are self-couplings of both Tx (coil) and Rx (coil) through the sample $\mathcal{L}_1$, $\mathcal{L}_2$ and a mutual coupling of Tx and Rx (coils) through the sample $\mathcal{M}$ (remote coupling). Hence, the previous equations are modified to take an account of the self-couplings of Tx and Rx (coils) through the sample, and the mutual coupling of Tx and Rx through the sample [34]. Hence, total inductance of Rx, $L = L_2 + \mathcal{L}_2$, mutual inductance of Tx and Rx probe M = M+ $\mathcal{M}$ and the internal resistance becomes of Rx r = r_2+ Δr_2. The Rx output voltage which is $V_O = R_L\, i_2$ becomes

$$Vo = (L_2 + \mathcal{M} + \mathcal{L}_2)\frac{di_2}{dt} + (r_2 + \Delta r_2)i_2 - M\frac{di_1}{dt} \quad (5)$$

From (5) we extract the impedance change due to the mutual coupling of the sample and PEC probe (6), direct mutual impedance of Tx and Rx (coils) (7) and self-impedance of the Rx (coil) (8) from output signal respectively as follows

$$\Delta Z = j\omega(\mathcal{M} + \mathcal{L}_2) + \Delta r_2 \quad (6)$$

$$Z_{TR} = j\omega M \quad (7)$$

$$Z = j\omega L_2 + r_2 \quad (8)$$

The impedance change due to the mutual coupling of the sample and probe ΔZ bears the information about the sample [32]. Whereas, Z_{TR}, the direct mutual impedance of Tx and Rx (coils), in addition to Rx (coil) self-impedance Z form an offset that masks the required information signal [11]. Because of the large value of the offset, the impedance change, the required information signal is a very small percentage of the Rx output voltage yielding a very low SNR output. As can be seen in (6)-(8), only ΔZ is the required information signal, Z_{TR} is the offset due to direct coupling of Tx (coil) and Rx (coil) whereas Z is the offset due to self-impedance of Rx (coil). Hence these two offsets are the main

sources of noise that limit SNR of the response signal. In our previous work [35], the problem of direct coupling Z_{TR} offset was mitigated. When a Tx-Rx PEC probe is in proximity of a conductive sample, the magnetic field of Tx (coil) couples directly with the Rx (coil) and forms an offset in Rx circuit. The Tx (coil) also couples indirectly through the sample with the Rx (coil) bearing the information about the test sample in the Rx circuit as in fig. 1b. Because the resultant value of these two couplings (M and $\mathcal{M}$) depend on coil gap and lift-off [32], we optimized coil gap and lift-off to minimize the offset (M) due to direct coupling of Tx and Rx (coils) . At the optimal lift-off, for every coil gap, the defect detection sensitivity was maximized.

Although the offset arising from direct coupling of Tx and Rx is eliminated, the offset due to self-impedance of the Rx (coil) is another challenge which this work propose to remove. As lift-off increases, the SNR decreases the more because the impedance change or the information signal generated by magnetic field of eddy current reaching the Rx (coil) diminishes whereas, the Rx (coil) self-impedance remains constant. Hence, at high lift-off, impedance change ΔZ becomes insignificant component of the output signal. Therefore, it is required to design a measurement circuit that can remove the effect of self-impedance of the Rx (coil) to improve SNR of the output signal. The next section explains the design and the principle of the proposed signal conditioning to achieve this requirement.

III. Proposed Signal Conditioning Circuit

The main idea of this paper is that high lift-off inspection is prone to noise. Therefore, we propose a signal conditioning that can improve SNR by removing the offset due to self-impedance of Rx (coil) which dominates the output signal. The proposed signal conditioning circuit is by modifying Maxwell's inductive bridge using opamp circuit to remove the self-impedance of Rx (coil) to improve SNR and linearity range at high lift-off. Hence, this section describes the modification and working of the proposed circuit. Maxwell's inductance bridge of Fig. 2a is modified using three high impedance and low-noise opamps, and passive components as in Fig. 2b. Inductors (coils) L2 and L3, and resistors R1 and R2 of Maxwell's inductance bridge form the feedback loops of two (opamps) A1 and A2 respectively which are working in inverting modes. A pulse excitation Ve is applied to the Tx (coil) which is coupled to two Rx (coils). The output of A_1 and A_2 are then fed into a subtractor opamp A_3 and output is measured as ΔV. The output voltages Va and Vb of opamps A_1 and A_2 are given by

$$V_a = -V_s \frac{r_3 + j\omega L_3}{R_1} \tag{9}$$

$$V_b = -V_s \frac{r_2 + j\omega L_2}{R_2} \tag{10}$$

Where L_2 and L_3, r_2 and r_3 are self-inductances and internal resistances of the feedback coils respectively. The voltage difference ΔV of the two outputs obtained at the output of op-amp A_3 is given by

$$\Delta V = \frac{V_s((r_3 + j\omega L_3)}{R_1} - \frac{(r_2 + j\omega L_2))}{R_2} \tag{11}$$

The complete Tx-Rx PEC probe circuit is configured as in Fig. 3a. Two coils L_2 and L_3 of the Rx circuit are coupled with the Tx (coil) above a test sample. The close proximity of Tx and Rx, in the presence of a sample, results in indirect coupling of Tx and Rx through the sample [34].Hence, as explained in section 2, the total self-inductance of Rx ($coil_2$) $= L_2 + \mathcal{L}_2$, and Rx ($coil_3$) $= L_3 + \mathcal{L}_3$, internal resistance of Rx ($coil_2$) $= r_2 + \Delta r_2$ and Rx ($coil_3$) $= r_3 + \Delta r_3$. Applying the push-pull configuration of the two Rx (coils), the mutual inductance of Tx and Rx ($coil_2$)$= M + \mathcal{M}$, mutual inductance of Tx and Rx ($coil_3$)$= -M - \mathcal{M}$. Also Self-inductance of Rx ($coil_2$) $= L_2 + \mathcal{L}_2$ and Rx ($coil_3$) $= L_3 - \mathcal{L}_3$. Substituting the changes in (11)

$$\Delta V = \frac{Vs(r_3 + \Delta r_3 + j\omega(L_3 + M + \mathcal{L}_3 + \mathcal{M}))}{R_1} - \frac{(r_2 + \Delta r_2 + j\omega(L_2 - M - \mathcal{L}_2 - \mathcal{M}))}{R_2} \tag{12}$$

If we choose $\Delta r_2 = \Delta r_3$, $R_2 = R_1 = R$, $r_2 = r_3$, $L_3 = L_2$, $\mathcal{L}_2 = \mathcal{L}_3 = \mathcal{L}$ and substitute in (12), the Rx output voltage becomes

$$\Delta V = \frac{Vs(2j\omega(M + \mathcal{L} + \mathcal{M}))}{R} \tag{13}$$

From (13), it can be seen that self-impedance of the Rx (coil) is suppressed from the output voltage. The offset due to direct coupling of Tx and Rx (coils) (M) can be eliminated as explained in Section II. Thereafter, the output signal ΔV becomes directly proportional to the impedance change of Rx (coils) ($\mathcal{L} + \mathcal{M}$). Hence, the output will be a minimum (ideally zero) without a sample. No offset output voltage will be present due to the self-impedance of the Rx (coil) or direct mutual impedance of Tx and Rx (coils).

At high lift-off as highlighted in section II, the change in impedance of Rx (coil) becomes insignificant compared to large Rx self-impedance. However, as the influence of Rx self-impedance has been removed by the conditioning circuit, the change in the impedance becomes a significant component of the output signal. Then, the output is fed to the computer (PC) via data acquisition system (DAS) for analog-to-digital conversion, digitization and low pass filtering which also reduces the effect of interference and noise on the output. Moreover, this configuration has a linear characteristic over a wide range of impedance change with improved sensitivity and stability.

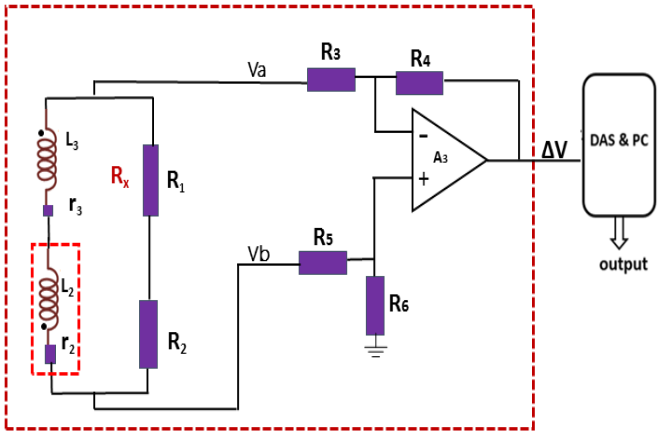

(a) Maxwell's inductive bridge

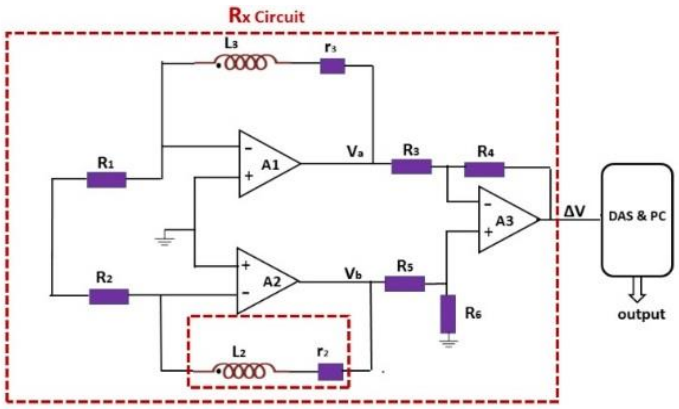

(b) Modified bridge circuit

Fig. 2. Different Signal Conditioning Circuit

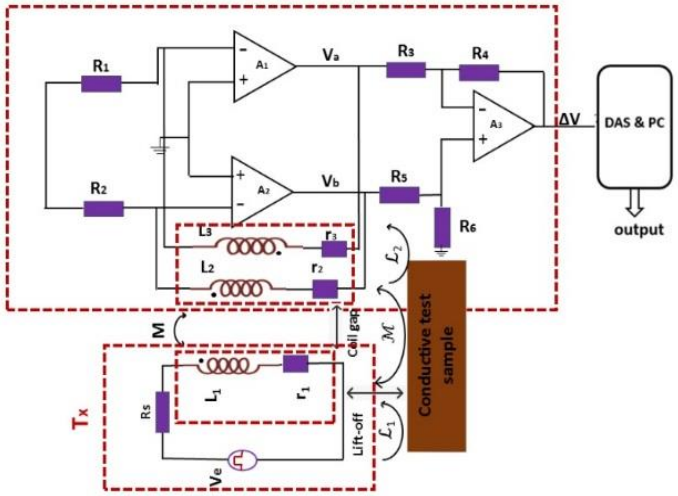

(a) Modified bridge conditioning circuit

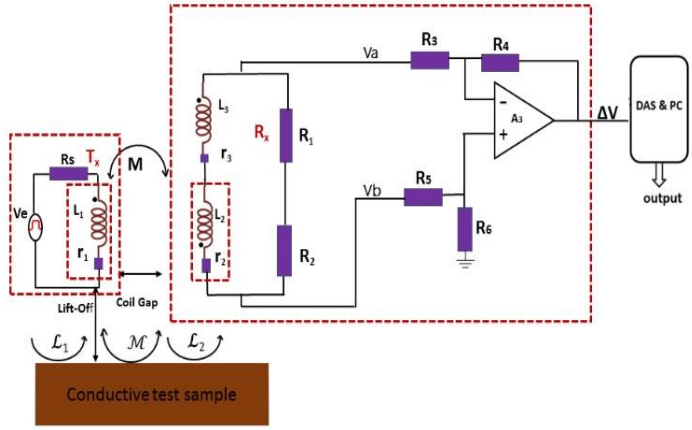

(b) Maxwell's inductive bridge conditioning circuit

Fig. 3. Tx-Rx probe above test sample with conditioning circuit

The improved linearity range of the modified circuit may be explained, thus; for identical coils in the modified circuit, the edge effects are assumed to be identical. Additionally, in the push-pull inductance measurement circuit of Fig. 3a, these edge effects cancel each other. Also, the non-inverting terminals of opamp A1 and A2 are connected to a common ground. Therefore, the inverting terminals are at the virtual ground where one end of the Rx (coils) are connected and stray capacitance between the terminals of the coils is negligible. The same excitation signal is an input to opamps A1 and A2 through input resistance R1 and R2. Hence, the other two terminals of the inductance coils are also at the same potential and the stray capacitance between these terminals is also negligible. The electromagnetic interference between the two Rx (coils) are similar and cancels each other when the differential voltages V1 and V2 are measured. Thus, the measurement error in the modified circuit is minimized. This is why the characteristic of the modified circuit is found to be quite linear even at high lift-off as reflected in the experimental results. However, the circuit may become unstable due to the derivative action and variations of the inductance in the feedback path. This instability can cause fluctuations of the output signal if the values of R1 and R2 are low. Increasing the resistances R1and R2 reduces the quality factors of the feedback circuits and enhances stability [36] but reducing sensitivity as can be seen in (13). Hence, R1 and R2 should be carefully chosen. Through series of experiments with different values of R1 and R2, 20k was chosen for both R1 and R2 in this work, to achieve a stabile output signal. As nodes Va and Vb are connected to the differential amplifier's input gain-setting resistors, the input resistors R3, R5 and R6 are selected to reduce the loading effect or directing current away from the bridge, which can affect the bridge output.

IV. Error Analysis

Equation (11) derived in section III considered that the proposed circuit elements possess ideal characteristics. However, practical devices used in the experiments such as opamps and resistors will poses non-ideal characteristics. The non-ideal characteristics of practical devices will give rise to errors in the output of the proposed circuit. Errors due to these non-idealities of the device elements and other factors are analyzed next.

A. Effects of Input Offset Voltages of A1, A2 and A3

A practical opamp used as A1 will possess a finite input offset voltage, Vs1. Hence Va will be at a potential Vs1, instead of virtual ground. As a result of this, Va will differ by an amount equal to Vs1. With this (9) will be modified as

$$V_a = (-V_s \frac{r_3 + j\omega L_3}{R_1}) \pm Vs1 \qquad (15)$$

Similarly, an input offset voltage Vs2 of opamp A2 will result in the potential Vb of A2 becoming Vs2 instead of being at virtual ground potential. Hence (10) will be modified as

$$V_b = (-V_s \frac{r_2 + j\omega L_2}{R_2}) \pm Vs2 \qquad (16)$$

Also, in addition to input offsets voltage of A1 and A2, the offset of A3, (Vs3) modifies (11) as

$$\Delta V = ((V_a \pm Vs1) - (V_b \pm Vs2)) \pm Vs3 \qquad (17)$$

Equations (15) to (17) indicate that the offset voltages of opamps used as A1, A2 and A3 directly affect the output. Hence, to minimize this error, opamps such as OPA277P possessing maximum input offset voltage of 20 μV have to be used as A_1, A_2 and A3.

B. Effects of Resistance tolerance

One of the conditions for the response given in equation (11) to give zero output in the absence of defect is that R1 = R2. Ideally, R1 may be equal to R2 but in reality it is not possible because of resistance mismatch. Also, equation (11) can be written as

$$\Delta V = \frac{R4}{R_3}(Vb - Va) \tag{18}$$

Hence the gain of A3 depends on the resistance values including R4 and R3. Although we can set the values of R4 and R3 to fix the gain, in reality the gain will vary due the resistance mismatch. This non-idealities generate offsets in the output and can alter the response signal. To minimize this error, matching resistances should be chosen in implementing the proposed circuit. To reduce error due to mismatch of R1 and R2, variable resistors can be used in place of R1 and R2 and by varying the two resistors the offset can be reduced before measurements are taken.

C. Electromagnetic field interference

One of the sources of errors of the proposed circuit is the interference on the inductive coils by outside electromagnetic fields. As in equation (13), the measurement parameter is mainly the mutual inductance due to the coupling of electromagnetic field of the coils and sample. The mutual inductance can be altered by external electromagnetic field which modifies equation (13) by coupling with the inductive coils with mutual inductance of $\mathcal{M}_{\text{out}}$. Hence (13) can modified by external electromagnetic field as

$$\Delta V = \frac{Vs\left(2j\omega(M + \mathcal{L} + \mathcal{M} \pm \mathcal{M}_{\text{out}})\right)}{R} \tag{19}$$

Equation (19) shows that the coupling of external electromagnetic field can alter the mutual inductance by $\mathcal{M}_{\text{out}}$ thereby causing measurement error. To reduce this error experimental setup should be shielded from electromagnetic interference. Errors due to stray capacitance between nodal points and ground can also contribute to measurement errors. However, the noninverting terminals of opamp A1 and A2 are connected to a common ground. Therefore, the inverting terminals are at virtual ground where one end of the Rx (coils) is connected and stray capacitance between these terminals of the coils is negligible.

V. EXPERIMENTAL SETUP

The experiment is carried out in three parts. In the first part, the influence of lift-off on Rx output voltage at a fixed coil gap with the Tx (coil) and Rx (coil) above the crack free aluminum sample without the conditioning circuit is studied. The variation of coil gap and lift-off is carried out with the help of the horizontal and vertical rulers attached to the plastic rack shown in the insets of Fig.4. The lift-off of Tx-Rx probe from the aluminum sample is increased from 0 mm to 55 mm at a step of 5 mm at fixed coil gaps of 1mm to 6mm at a step of 1mm and at each step the amplitude of the Rx output voltage is read and recorded with an oscilloscope. Although the expected lift-off is 30mm, we extended the study to 55mm so that we can observe whether the Rx output converges to its value when there is no sample. In the second part, lift-off variation is studied with the Maxwell's inductive bridge by varying the lift-off and coil gap as explained in the first part. Also the lift-off influence of the modified bridge is studied by repeating the same procedure as used in Maxwell's inductance bridge.

In the third part, the performance of the modified circuit and Maxwell's inductance bridge with crack detection in the aluminum sample is studied. The probe is used to scan at the steps of 2.5 mm for 30 scan points along the aluminum sample with a crack. At each scan point, the value of Rx output voltage is read and recorded. The peak values of reference subtracted Rx output voltage is then plotted against the scan points. The values of circuit parameters used are L1 = L2 = L3 = 10.7uH, $r_1 = r_2 = r_3 = 0.2$ohms, R1 = R2= 20k, R3 = R5 = 1k, R4 = R6 = 10k, (R1-R6) with tolerance of 5%. A1= A2 = A3 = 741 opamp. The Experimental setup and the block diagram of materials used is in Fig.4. The PEC probe including signal generator, oscilloscope, one Tx (coil) and two Rx (coils) are connected as in Fig. 4a. Pulse signal of amplitude 4 V, pulse width 20us, frequency 4 kHz was supplied to the Tx circuit and amplitude of the output of the Rx (coil) is read and recorded. An excitation frequency of 4 kHz was chosen considering the maximum Tx-Rx probe response signals observed on the surface of the crack within the range of lift-off and coil gap used in the experiment [43, 44]. Aluminum Sample measuring 400 mm x 50 mm x 50 mm is used for both lift-off influence study and for crack detection. Rx (coil) is identical to Tx (coil), a rectangular coil with an inner diameter 12 mm, outer diameter 25 mm, length 36 mm and 15 turns.

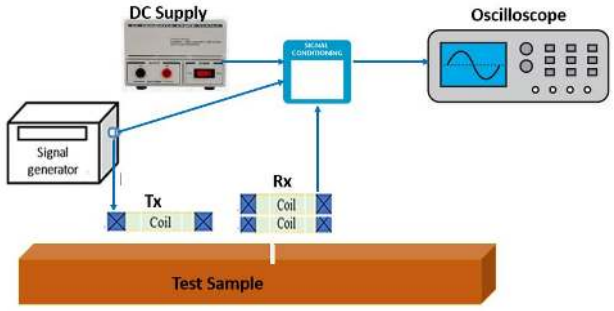

(a) Block diagram

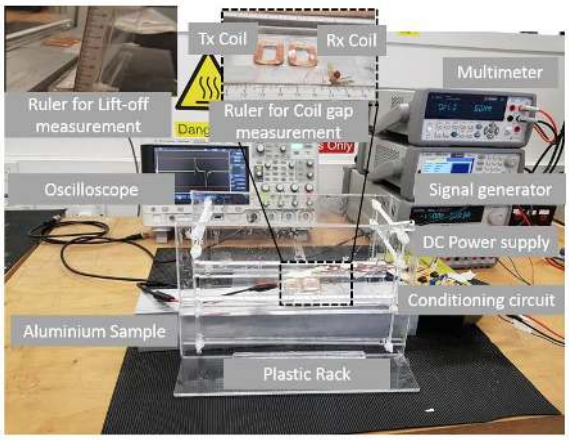

(b) Instruments and sample Setup

Fig. 4. Experimental setup

VI. Experimental Results and Discussions

Based on the experimental setups and procedures described in the previous section, we collected measurement data from each experiment. In this section, the results of the experiments are discussed under lift-off influence and linearity, sensitivity to crack detection and SNR, and comparison of the conditioning circuits.

A. Lift-off Influence and linearity range

In this section, we explain how lift-off variation affects the linearity of the input-output characteristic of the Tx-Rx PEC probe without conditioning circuits, with the modified circuit and with Maxwell's inductance bridge circuit. The response of the Rx circuit with pulse signal is in Fig. 5. We extracted the amplitude of the response signal for every lift-off variation. The ideal (probe without conditioning circuit) static characteristic curve of the Tx-Rx (coils) in Fig. 6a reveals a good linearity response. It can be observed that there is relative linearity from 0mm to 55 mm lift-off. Hence, PEC testing in the lift-off range will not be affected by non-linearity. However, the large value of the self-impedance (offset) of Rx (coil) made amplitude of the output signal very high compared to those with conditioning circuit. The static characteristic curve for the modified circuit in Fig. 6b depicts almost the same linearity as that of Fig. 6a.Therefore, at the same lift-off, PEC testing of Fig. 6b the little linearity deviation from that of Fig. 6a. The static characteristic curve of the Maxwell's inductance bridge circuit in Fig. 6c depicts good linearity at a low lift-off but as the lift-off increases to about 15 mm, non-linearity sets in, as reflected in the zigzag nature of the graph. The nonlinearity exists at higher lift-off due to the limited linearity range of Maxwell's bridge circuit. Hence, PEC testing can only be taken without measurement errors at lift-off lower than 15 mm with Maxwell's bridge conditioning circuit. Whereas that of the modified circuit is extended to about 50 mm.

The percentage deviations from the linearity of Maxwell's inductance bridge and the modified circuit for different coil gaps are in Fig. 7. The deviation of the modified circuit Fig.7b is found to be smaller than that of Maxwell's inductance bridge Fig. 7a for coil gaps 1mm to 6mm as shown in the boxes on the graphs. From this, it can be concluded that the modified circuit has a better linearity range and characteristics than convectional Maxwell's bridge circuit. Figs. 8a and 8b show curves and error bars of the measured data of eight repeated experiments with both Maxwell's bridge circuit and the modified circuit.

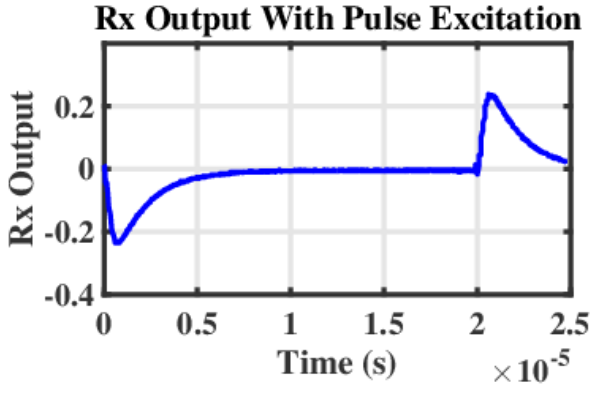

Fig. 5. Response signal of Rx with repeated pulse excitation of Tx

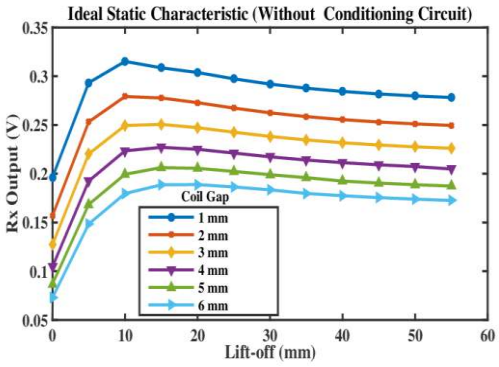

(a) Ideal

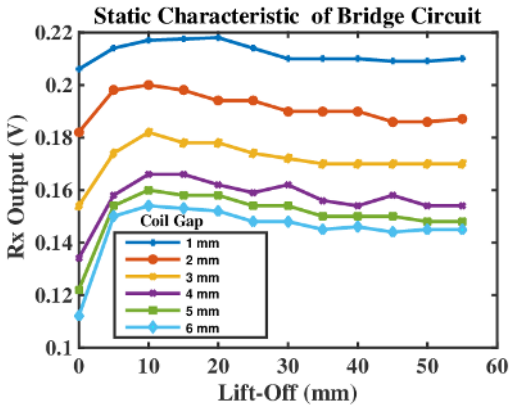

(b) bridge circuit

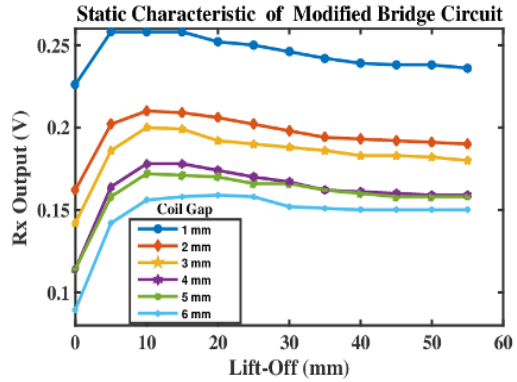

(c) Modified circuit

Fig.6. Static characteristic curve of Tx-Rx probe

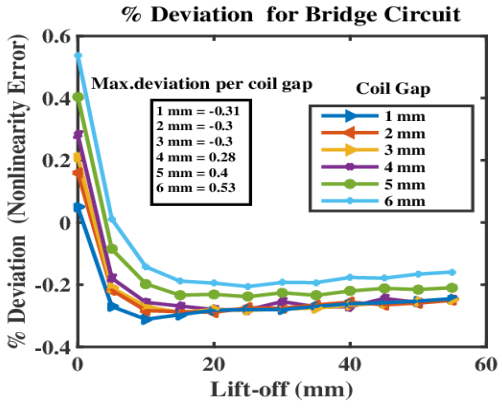

(a) Maxwell's inductance circuit

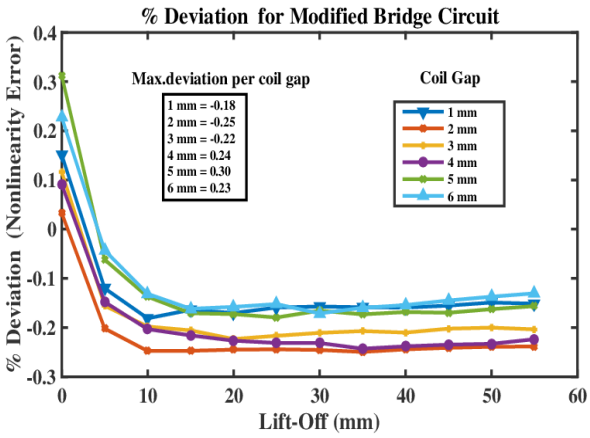

(b) Modified circuit

Fig. 7. Percentage deviation from the ideal linearity

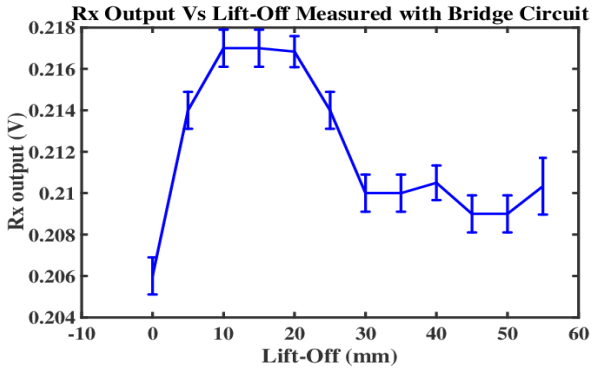

(a) Maxwell's inductance bridge

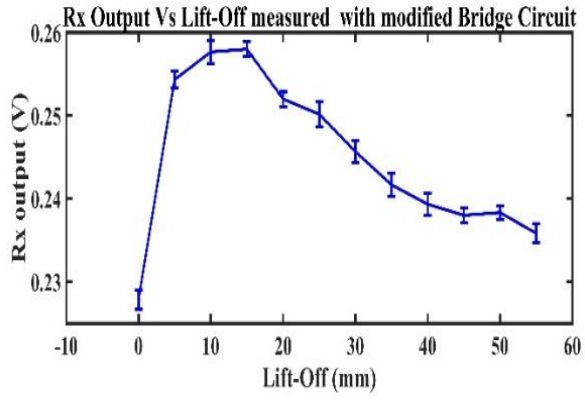

(b) Modified circuit

Fig. 8 Measurement errors of the Circuits

B. Sensitivity to crack detection and SNR

In this subsection, we discuss an application of the proposed circuit in surface crack detection of an aluminum sample and compare its performance with conventional Maxwell's inductance bridge in sensitivity and SNR. The modified circuit and Maxwell's inductance bridge are used for artificial crack detection in the aluminum sample. At a fixed coil gap of (4 mm) and lift-off (30 mm), the aluminum sample is scanned with a Tx-Rx probe and the Rx output voltage is read and recorded as described in section IV. The peak values of reference subtracted output voltage of the Rx (coil) connected to the modified circuit and Maxwell's inductance bridge one after the other are plotted in Fig. 8. It can be observed that the two circuits show a different response shape due to the crack influence. Whereas, the response of Maxwell's bridge forms a trough (negative peak), the response of the modified circuit peaks as Tx (coil) passes over a crack. The crack is detected by the Tx (coil) between 10 mm to 30 mm of the scan distance. After a transition of the crack from the Tx (coil) to Rx (coil) at scan distance of 30 mm to 45 mm, the Rx (coil) detects the crack with a peak for both circuits. However, considering sensitivity in amplitude change, it can be observed that with Tx (coil) detection of the crack the amplitude of the response signal changes from 12.5 mV to 0 mV for Maxwell's inductance bridge whereas that of modified circuit changes from 0 mV to 27 mV. For Rx detection, the amplitude changes from 6 mV to 15 mV with Maxwell's inductance bridge, whereas that of the modified circuit changes from 6 mV to 29.5 mV. Hence, the change in amplitude for Tx and Rx (coil) of the modified circuit is far greater than that of Maxwell's inductance bridge. Therefore, we conclude that the modified circuit has better sensitivity to crack than Maxwell's inductance bridge. However, it is easier to build a relationship between the extracted amplitude feature, and the detected crack with Maxwell's inductance bridge than the modified circuit based on crack response shape. For instance, there are two troughs and two peaks in Maxwell's inductance bridge response which simply signifies one peak and one trough each for Tx and Rx respectively. In the modified circuit response, there are three peaks and two troughs which are more difficult to map with the crack geometry. Hence, it is easier to characterize crack with Maxwell's inductance bridge than the modified circuit.

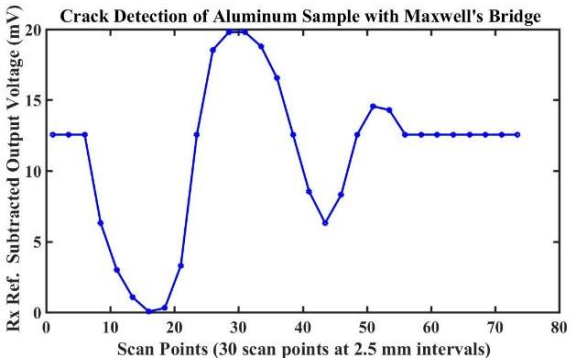

(a) Maxwell's Inductance Bridge

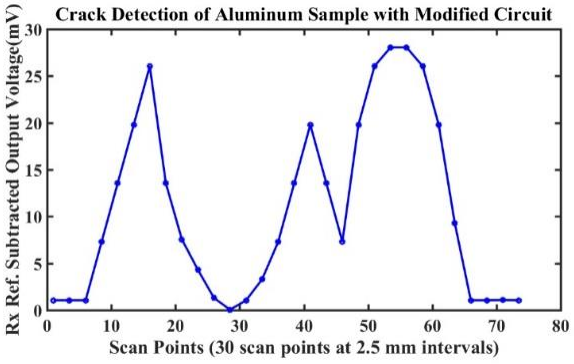

(b) Modified Circuit

Fig. 9. Crack detection of the aluminum sample

To explain how the circuits perform in SNR, we define

SNR as a ratio of the impedance change due to the presence of a crack to the output signal. Lift-off noise, self-impedance, the direct mutual impedance of Tx and Rx (coils) (offset), and impedance change due to crack on the sample are the components of the output signal. Hence, on the surface of a sample, the output signal is the offset superimposed on the impedance change [37]. Because analysis and quantification of defects mainly depend on the impedance change, the offset signal is equivalent to noise. Hence, signal-to-noise ratio (SNR) is defined as

$$SNR = \frac{Max(Vc)}{Max(Vnc)} \quad (14)$$

Where Max (Vc) and Max (Vnc) are the maximum values of output signal of the sample with and without crack.

TABLE I
THE EXPERIMENTAL SNR OF MAXWELL'S BRIDGE AND MODIFIED CIRCUIT.

	Maxwell bridge(mV)	Modified Circuit (mV)
Without Crack	318.5	207.75
With Crack	511.5	572.25
SNR	1.61	2.75

From table 1, it is clear that the proposed signal conditioning circuit has higher SNR which signifies higher sensitivity to crack than the conventional Maxwell's inductance bridge.

C. *Performance Comparison.*

The modified circuit has higher SNR and sensitivity to crack detection, especially at high lift-off compared to conventional Maxwell's inductance bridge. However, it is easier to build a link between amplitude features of the output signal crack geometries with Maxwell's inductance bridge than the modified circuit. The modified circuit in comparison to related works as in table II also shows improved linearity performance.

TABLE II
PERFORMANCE COMPARISON OF PROPOSED CIRCUIT WITH LITERATURE WORKS.

Circuit	Linearity Error (%)	Circuit configuration
proposed circuit	0.18	Simple and low cost
[38, 39]	2	complex
[40]	0.3	Digital ,but with added cost
[41]	0.4	unstable
[19]	1	simple
[42]	0.2	complex

VII. CONCLUSION AND FURTHER WORK

A modified Maxwell's inductance bridge based on the opamp circuit of Tx-Rx PEC probe is proposed and investigated for high lift-off PEC testing. The analysis of three performance metrics of SNR, linearity range and sensitivity at high lift-off for the new signal conditioning circuit has been carried out. It is shown that the modified circuit has a higher SNR of 2.75 against 1.61 for bridge circuit for coil gap 4 mm and lift-off 20 mm. The lift-off linearity range for the modified circuit is 0 mm to 55 mm whereas the bridge has 0 mm to 15 mm. The crack detection by Tx (coil) based on amplitude change is found to be 27 mV for modified circuit against 12.5 mV for bridge circuit while that of Rx (coil) detection is 23.5 mV for the modified circuit against 9 mV for bridge circuit. However, it is easier to build a relationship between crack geometry and bridge response based on crack influence shapes than the modified circuit. Also as a result of the modifications, a large impedance change can be measured and amplified by the signal conditioning circuit as self-impedance of Rx (coil) has been suppressed. Small linearity range of conventional Maxwell's bridge circuit is extended with improved sensitivity. The modified circuit hence has good measurement accuracy. Finally, the circuit becomes much simpler and cost-effective and no bridge balancing is needed.

Further work on the modified circuit is underway for the quantification of crack geometry with appropriate feature extraction, and selection for quantitative nondestructive evaluation (QNDE) and long term stability.

ACKNOWLEDGMENT

The author acknowledges the support by the Tertiary Education Trust Fund (TET Fund) Nigeria.

REFERENCES

[1] C. Huang, X. Wu, Z. Xu, and Y. Kang, "Ferromagnetic material pulsed eddy current testing signal modeling by equivalent multiple-coil-coupling approach," *NDT & E International,* vol. 44, no. 2, pp. 163-168, 2011.

[2] X. Chen, and Y. Lei, "Excitation current waveform for eddy current testing on the thickness of ferromagnetic plates," *NDT & E International,* vol. 66, pp. 28-33, 2014.

[3] C. Jiabao, and W. Haibo, *pulse eddy current nondestructive testing.*: Topics in Chemical & Material Engineering, 1 (1) :351-353. , 2018.

[4] N. Ulapane, A. Alempijevic, T. Vidal Calleja, and J. Valls Miro, "Pulsed eddy current sensing for critical pipe condition assessment," *Sensors,* vol. 17, no. 10, pp. 2208, 2017.

[5] A. S. Repelianto, and N. Kasai, "The Improvement of Flaw Detection by the Configuration of Uniform Eddy Current Probes," *Sensors,* vol. 19, no. 2, pp. 397, 2019.

[6] L. Obrutsky, B. Lepine, J. Lu, R. Cassidy, and J. Carter, "Eddy current technology for heat exchanger and steam generator tube inspection," *Proc. 16th WCNDT, Montreal (Canada),* vol. 30, 2004.

[7] W. Li, Y. Ye, K. Zhang, and Z. Feng, "A thickness measurement system for metal films based on eddy-current method with phase detection," *IEEE Transactions on Industrial Electronics,* vol. 64, no. 5, pp. 3940-3949, 2017.

[8] Z. Qu, Q. Zhao, and Y. Meng, "Improvement of sensitivity of eddy current sensors for nano-scale thickness measurement of Cu films," *NDT & E International,* vol. 61, pp. 53-57, 2014.

[9] M. Jagiella, S. Fericean, and A. Dorneich, "Progress and recent realizations of miniaturized inductive proximity sensors for automation," *IEEE sensors journal,* vol. 6, no. 6, pp. 1734-1741, 2006.

[10] V. Gunasekaran, B. George, S. Aniruddhan, D. D. Janardhanan, and R. V. Palur, "Performance Analysis of Oscillator-Based Read-Out Circuit for LVDT," *IEEE Transactions on Instrumentation and Measurement*, no. 99, pp. 1-9, 2018.

[11] R. R. Robaina, H. T. Alvarado, and J. A. Plaza, "Planar coil-based differential electromagnetic sensor with null-offset," *Sensors and Actuators A: Physical,* vol. 164, no. 1-2, pp. 15-21, 2010.

[12] M. R. Nabavi, and S. Nihtianov, "Eddy-current sensor interface for advanced industrial applications," *IEEE Transactions on Industrial Electronics,* vol. 58, no. 9, pp. 4414-4423, 2010.

[13] H. Zhang, M. Zhong, F. Xie, and M. Cao, "Application of a Saddle-Type Eddy Current Sensor in Steel Ball Surface-Defect Inspection," *Sensors,* vol. 17, no. 12, pp. 2814, 2017.

[14] H. Wang, Y. Liu, W. Li, and Z. Feng, "Design of ultrastable and high resolution eddy-current displacement sensor system." pp. 2333-2339.

[15] H. Wang, and Z. Feng, "Ultrastable and highly sensitive eddy current displacement sensor using self-temperature compensation," *Sensors and Actuators A: Physical,* vol. 203, pp. 362-368, 2013.

[16] G. Y. Tian, Z. X. Zhao, R. W. Baines, and P. Corcoran, "Blind sensing [eddy current sensor]," *Manufacturing Engineer,* vol. 76, no. 4, pp. 179-182, 1997.

[17] G. Y. Tian, *Eddy current frequency output sensors for precision engineering*, 2001.

[18] Z. Liu, A. D. Koffman, B. C. Waltrip, and Y. Wang, "Eddy current rail inspection using AC bridge techniques," *Journal of research of the National Institute of Standards and Technology,* vol. 118, pp. 140, 2013.

[19] S. Chattopadhyay, and S. C. Bera, "Modification of the Maxwell–Wien Bridge for Accurate Measurement of a Process Variable by an Inductive Transducer," *IEEE Transactions on Instrumentation and Measurement,* vol. 59, no. 9, pp. 2445-2449, 2010.

[20] A. D. Marcellis, C. Reig, and M. Cubells-Beltrán, "Current-Based Measurement Technique for High Sensitivity Detection of Resistive Bridges With External Balancing Through Control Voltages," *IEEE Sensors Journal,* vol. 17, no. 2, pp. 404-411, 2017.

[21] P. R. Nagarajan, B. George, and V. J. Kumar, "A Linearizing Digitizer for Wheatstone Bridge Based Signal Conditioning of Resistive Sensors," *IEEE Sensors Journal,* vol. 17, no. 6, pp. 1696-1705, 2017.

[22] S. Chattopadhyay, B. R. Maity, and S. Pal, "Accurate measurement of'Q'factor of an inductive coil using a modified maxwell wein bridge network," *Sensors & Transducers,* vol. 105, no. 6, pp. 10, 2009.

[23] C. Baby, and B. George, "A simple analog front-end circuit for grounded capacitive sensors with offset capacitance." pp. 1372-1375.

[24] S. Malik, T. Islam, K. Kishore, K. Kumar, S. A. Akbar, and B. A. Botre, "A simple analog interface for capacitive sensor with offset and parasitic capacitance." pp. 1-4.

[25] N. Mandal, and G. Rajita, "An accurate technique of measurement of flow rate using rotameter as a primary sensor and an improved op-amp based network," *Flow Measurement and Instrumentation,* vol. 58, pp. 38-45, 2017.

[26] G. Spiezia, R. Losito, M. Martino, A. Masi, and A. Pierno, "Automatic test bench for measurement of magnetic interference on LVDTs," *IEEE Transactions on Instrumentation and Measurement,* vol. 60, no. 5, pp. 1802-1810, 2011.

[27] G. Klein, J. Morelli, and T. W. Krause, "Analytical model of the eddy current response of a drive-receive coil system inside two concentric tubes," *NDT & E International,* vol. 96, pp. 18-25, 2018.

[28] M. S. Luloff, J. Morelli, and T. W. Krause, "Examination of Dodd and Deeds solutions for a transmit-receive eddy current probe above a layered planar structure." p. 110004.

[29] M. E. Ibrahim, and S. K. Burke, "Mutual Impedance of Eddy-Current Coils Above a Second-Layer Crack of Finite Length," *Journal of Nondestructive Evaluation,* vol. 38, no. 2, pp. 50, 2019.

[30] F. Mocholí Belenguer, A. Mocholí Salcedo, V. Milián Sánchez, and J. H. Arroyo Núñez, "Double Magnetic Loop and Methods for Calculating Its Inductance," *Journal of Advanced Transportation,* vol. 2018, 2018.

[31] X. Sheng, Y. Li, M. Lian, C. Xu, and Y. Wang, "Influence of Coupling Interference on Arrayed Eddy Current Displacement Measurement," *Materials Evaluation,* vol. 74, no. 12, pp. 1675-1683, 2016.

[32] W. Dehui, H. Tianfu, W. Xiaohong, and S. Lingxin, "Analytical model for mutual inductance between two rectangular coils in driver pickup mode for eddy current testing," *Nondestructive Testing and Evaluation,* vol. 33, no. 1, pp. 20-34, 2018.

[33] L. Xie, B. Gao, G. Y. Tian, J. Tan, B. Feng, and Y. Yin, "Coupling pulse eddy current sensor for deeper defects NDT," *Sensors and Actuators A: Physical,* vol. 293, pp. 189-199, 2019.

[34] D. Desjardins, T. W. Krause, and L. Clapham, "Transient response of a driver-pickup coil probe in transient eddy current testing," *NDT & E International,* vol. 75, pp. 8-14, 2015.

[35] D. I. Ona, G. Y. Tian, R. Sutthaweekul, and S. M. Naqvi, "Design and optimisation of mutual inductance based pulsed eddy current probe," *Measurement,* vol. 144, pp. 402-409, 2019/10/01/, 2019.

[36] G. R. Guerreiro, and J. Navarro, "Design for stability of active inductor with feedback resistance." pp. 1-6.

[37] S. K. Burke, and M. E. Ibrahim, "Mutual impedance of air-cored coils above a conducting plate," *Journal of Physics D: Applied Physics,* vol. 37, no. 13, pp. 1857, 2004.

[38] A. De Marcellis, G. Ferri, and P. Mantenuto, "Analog Wheatstone bridge-based automatic interface for grounded and floating wide-range resistive sensors," *Sensors and Actuators B: Chemical,* vol. 187, pp. 371-378, 2013.

[39] P. Mantenuto, A. De Marcellis, and G. Ferri, "Uncalibrated analog bridge-based interface for wide-range resistive sensor estimation," *IEEE Sensors Journal,* vol. 12, no. 5, pp. 1413-1414, 2011.

[40] E. Sifuentes, O. Casas, F. Reverter, and R. Pallas-Areny, "Direct interface circuit to linearise resistive sensor bridges," *Sensors and Actuators A: physical,* vol. 147, no. 1, pp. 210-215, 2008.

[41] G. De Graaf, and R. F. Wolffenbuttel, "Systematic approach for the linearization and readout of nonsymmetric impedance bridges," *IEEE transactions on instrumentation and measurement,* vol. 55, no. 5, pp. 1566-1572, 2006.

[42] V. Stornelli, G. Ferri, A. Leoni, and L. Pantoli, "The assessment of wind conditions by means of hot wire sensors and a modifed Wheatstone bridge architecture," *Sensors and Actuators A: Physical,* vol. 262, pp. 130-139, 2017/08/01/, 2017.

[43] M. Fan, Q. Wang, B. Cao, B. Ye, A. Sunny, and G. Tian, "Frequency optimization for enhancement of surface defect classification using the eddy current technique," *Sensors,* vol. 16, no. 5, pp. 649, 2016.

[44 Y. Yating, and G. Jia, "Investigation of signal features of pulsed eddy current testing technique by experiments," *Insight-Non-Destructive Testing and Condition Monitoring,* vol. 55, no. 9, pp. 487-491, 2013.

Denis Ijike Ona received B.Eng. and M.Eng. Degrees in Electrical Engineering from Nnamdi Azikiwe University, Nigeria, in 2002 and 2012 respectively. He joined the Electrical Engineering Department of Akanu-Ibiam Fed. Polytechnic Unwana in 2009 as academic staff. Mr. Ona is currently pursuing a PhD degree in Electrical and Electronic Engineering at the School of Engineering, Newcastle University, UK. His main research interest is electromagnetic sensing for nondestructive testing and evaluation (NDT&E).

Gui Yun Tian (M'01–SM'03) received the B.Sc. degree in metrology and instrumentation and M.Sc. degree in precision engineering from the University of Sichuan, Chengdu, China, in 1985 and 1988, respectively, and the Ph.D. degree from the University of Derby, Derby, U.K., in 1998. He was a Lecturer, a Senior Lecturer, a Reader, a Professor, and the Head of the Group of Systems Engineering, University of Huddersfield, UK, from 2000 to 2006. Since 2007, he has been with Newcastle University, Newcastle upon Tyne, U.K., where he is a Chair Professor of sensor technologies. Currently, he is also an Adjunct Professor with the School of Automation Engineering, University of Electronic Science and Technology of China. He has coordinated several research projects with the Engineering and Physical Sciences Research Council, the Royal Academy of Engineering, and FP7. He has also collaborated with leading industrial companies such as Airbus, Toulouse, France, Rolls Royce, Derby, U.K., BP, London, U.K., nPower, Swindon, U.K., and TWI.

Syed Mohsen Naqvi (S'07-M'09-SM'14) received the Ph.D. degree in Signal Processing from Loughborough University, Loughborough, U.K., in 2009 and his Ph.D. thesis was on the EPSRC U.K. funded project. He was a Postdoctoral Research Associate on the EPSRC U.K. funded projects and REF Lecturer from 2009 to 2015. Prior to his postgraduate studies in Cardiff and Loughborough Universities U.K., he served the National Engineering and Scientific Commission (NESCOM) of Pakistan from 2002 to 2005.

Dr Naqvi is Lecturer/Assistant Professor in Signal and Information Processing at the School of Engineering, Newcastle University, and Newcastle, U.K. His current research interests include multimodal processing for human behavior analysis, multi-target tracking, and source separation; all for machine learning. He organized special sessions in FUSION, delivered seminars and was a speaker at UDRC Summer Schools 2015-2017. He has above 100 publications with the main focus of his research being on Multimodal (audio-video) Signal and Information Processing. He is an Associate Editor for Elsevier Journal on Signal Processing. He is Fellow of the Higher Education Academy (FHEA).He is an Associate Editor for IEEE Transactions on Signal Processing.